

Studies on the Formation and Characteristics of Two Types of *p*-Xylene/Silicalite-1 Associates

YINGCAI LONG,* YAOJUN SUN², HONG ZENG¹, ZI GAO¹,
TAILIU WU² and LIPING WANG²

¹Department of Chemistry, Fudan University, Shanghai 200433, P.R. China.

²Center of Analysis and Measurement, Fudan University, Shanghai 200433, P.R. China.

(Received: 24 October 1995; in final form: 13 November 1996)

Abstract. High resolution ²⁹Si MAS NMR, ¹³C CP MAS NMR, and TG/DTG/DTA were used to study the interaction between the framework of siliceous MFI type zeolite (silicalite) and the adsorbed *p*-xylene. The zeolite sample used in this study possesses a perfect framework. A series of high resolution ²⁹Si MAS NMR and ¹³C CP MAS NMR spectra of the samples with various loadings of *p*-xylene were measured. Experimental results of XRD, NMR and thermal analysis confirm the formation of two types of *p*-xylene/silicalite associate. The properties of the two types of associates are given in terms of their XRD patterns, NMR spectra and TG/DTG/DTA curves. When the *p*-xylene loading is less than four molecules per unit cell, the adsorbed molecules disperse in the sinusoidal channels and interact with the framework O²⁻ forming associate-I (*p*-xylene/silicalite), and inducing the monoclinic/orthorhombic(I) transition. When the *p*-xylene loading is more than 5.2 molecules/u.c., the adsorbed *p*-xylene molecules are located in the channel intersections and combined into a *p*-xylene/*p*-xylene complex via hydrogen bonding, forming associate-II (*p*-xylene/*p*-xylene/silicalite) and inducing the orthorhombic(I)/orthorhombic(II) transition. The desorption of *p*-xylene from associate-II occurs at about 90 °C with an evident endothermic effect, whereas the desorption from associate-I occurs at about 140 °C without any visible heat effect, implying that two types of sorption and desorption processes exist in this host/guest system.

Key words: Host/guest interaction, associate, silicalite-1, *p*-xylene, XRD, ²⁹Si MAS NMR, ¹³C CP MAS NMR, TG/DTG/DTA.

1. Introduction

MFI type zeolite is a hydrophobic zeolite and has wide applications in catalysis and separation. There are many publications related to its structure, adsorption and desorption. Among the adsorbates usually investigated, hexane and other *n*-alkanes, and aromatics such as benzene, toluene, *p*-xylene are the most common [1–7].

Water sorption by the zeolite has been shown to vary linearly with aluminum content [1]. The saturated sorption capacities of hydrocarbons are different in Al-free ZSM-5, Na-ZSM-5, K-ZSM-5 [3], and are greatly influenced by zeolite crystal size and aluminum content [5, 8]. The silanol groups in siliceous ZSM-5(silicalite) increase the heat of sorption of 2-butyne by 10 KJ/mol compared with the heat of

* Author for correspondence.

sorption of *n*-butane [9]. It was found that the solid phase changes from 4 to 6.5 molecules of *p*-xylene adsorbed per unit cell of ZSM-5 [2]. An unusual hysteresis in the adsorption isotherm of *p*-xylene is caused by unusual sorbent/sorbate or sorbate/sorbate interactions [6]. The formation of a bromobenzene complex was found by calorimetry [10]. Molecular dynamics simulation of propane and methane in silicalite indicated both adsorbate/silicalite and adsorbate/adsorbate interactions [7]. The sorption energy in both *n*-alkanes–silicalite and in *p*-xylene–silicalite systems have also been calculated by computer simulations [11, 12]. The most important work was the determination of the location of *p*-xylene in a single crystal of zeolite H-ZSM-5 [13]. The nature of interaction forces between the methyl(H) atom in a xylene and the aromatic ring atoms in a neighbor xylene was reversed. XRD and NMR studies revealed the inconvertible symmetry transition of siliceous MFI zeolite at low loadings of *p*-xylene, benzene, pyridine and acetylacetone [14–16]. The unusual features on sorption isotherms and on TPD(TG)/DTG curves of *n*-hexane and heptane were found to be caused by a commensurate freezing in silicalite, with a kind of phase transition taking place [17, 18].

The essential host/guest interaction can be clearly studied on the perfect framework of silicalite. The affinity order of 27 organic compounds with different functional groups has been compared in terms of the A_T value determined by DTG [19–21]. The sorbate/framework and sorbate/sorbate interactions for certain organics were found from the double peaks on the DTG curves and thermal effects on DTA curves [22]. A multi-molecule complex is found to form in silicalite with *p*-xylene, toluene, phenol, ethylene glycol, and ethylamine. A phase transition is caused by the different filling in zig zag channels with various lengths of alkanes and alkylamines.

It is well known that the framework symmetry of MFI type zeolite is quite flexible. In general, the as-synthesized MFI zeolite has an idealized orthorhombic symmetry, which changes to monoclinic symmetry after certain treatments, such as calcination and ion exchanges [23]. The transition between orthorhombic and monoclinic symmetry is reversible. The monoclinic symmetry calcined silicalite may change to orthorhombic at elevated temperatures, and the temperature of the monoclinic/orthorhombic transition is influenced by the nature of the cations and the aluminum content in the zeolite [23, 24]. The monoclinic/orthorhombic transition is also induced by adsorbing certain chemical species [14, 25]. In addition the silicalite synthesized with tetrapropylammonium ion (TPA) as a template presents a transition from orthorhombic to monoclinic form as the sample is cooled to a temperature of about 175 K [26]. XRD and high resolution ^{29}Si MAS NMR are powerful techniques for the identification of such kinds of symmetry transition. X-ray single crystal structural analysis results show that there are three space groups of MFI zeolite: $Pnma$ (orthorhombic symmetry) for as-synthesized ZSM-5 [27], $P2_1/n$ (monoclinic symmetry) for H-ZSM-5 [28], and $P2_12_12_1$ (orthorhombic symmetry) for the *p*-xylene/H-ZSM-5 complex [13]. The ultra-high resolution ^{29}Si MAS NMR spectrum of highly siliceous MFI zeolite(silicalite) exhibits clearly

resolved resonances for 21 of the 24 postulated lattice sites in the network of monoclinic symmetry [29, 30].

Recently, silicalite has been used as an effective shape-selective adsorbent for the separation of the isomers of C₈ aromatics in the petrochemical industry. The sorption and desorption behaviors of silicalite are very different from those of its aluminum bearing analogues [20, 31]. It is interesting to have found that there are two orthorhombic symmetries with different loadings of *p*-xylene in such a system, as revealed by XRD. When the loading is < 4 molecules per unit cell(u.c.), the *M*(monoclinic, *P*2₁ group) symmetry changes to *O*₁ (orthorhombic, *Pnma* group). After saturation (8 molecules/u.c.), the *O*₁ → *O*₂ (orthorhombic, *P*2₁2₁2₁ group) transition is achieved [16, 23]. Therefore, we estimate that there are two types of *p*-xylene/silicalite complex formed. In this work the formation process and the structure of these complexes will be studied in detail by XRD, ²⁹Si and ¹³C MAS NMR, and TG/DTG/DTA methods. We will discuss the experimental results in terms of the host/guest interactions.

2. Experimental

2.1. PREPARATION

The silicalite sample used in this study was hydrothermally synthesized in an ethylamine–Na₂O–SiO₂–H₂O system using water glass as a source of silicon [32]. The as-synthesized zeolite product was washed, filtered, dried, and then calcined in an oven to remove the organic template at about 600 °C for 2 h. It was then treated with 0.5N HCl solution at 95 °C for 4 h and washed, filtered, dried and calcined at 550 °C for 2 h. Finally, the zeolite was further dealuminated at 800 °C for 100 h in a flow of air saturated with water vapour.

The SEM microphoto shows the silicalite sample is in a prismatic form of single crystals up to the size of 6 × 15 μm. ²⁹Si MAS NMR spectra show that the Si-OH peak at –103 ppm and Si(1Al) peak at –106 ppm disappear. The *n*-hexane sorption volume is 0.182 ml/g (~8.0 molecules/u.c.) at *P*/*P*₀ = 0.5 measured by adsorption isotherms at 25 °C. The water sorption is 0.4 wt% at *P*/*P*₀ = 0.8. The BET and the Langmuir surface area of the sample are 380.2 m²/g and 532.3 m²/g, respectively, measured by N₂ sorption at 77 K. The pore volume is 0.1828 mL/g calculated from the N₂ sorption isotherm at *P*/*P*₀ = 0.9744. These sorption data indicate that the silicalite sample has an ideal porous system, consistent with references [1, 2, 7, 18, 34]. Its crystallinity is 100%. The quality of the sample is good enough for the investigation in this study.

The dry silicalite-1 was kept over liquid *p*-xylene in a desiccator at ambient temperature for 2 to 200 h to obtain samples with various loadings of *p*-xylene.

2.2. CHARACTERIZATION

XRD patterns were collected at room temperature using a D-MAX/II A X-ray powder diffractometer with $\text{CuK}\alpha$ radiation in the 2θ range of $5\text{--}50^\circ$ at a scanning speed of $8^\circ(2\theta)/\text{min}$, and in the 2θ range of $22\text{--}25^\circ$, $29\text{--}31^\circ$, $44\text{--}46^\circ$, and $48\text{--}50^\circ$ at a scanning speed of $0.5^\circ(2\theta)/\text{min}$. ^{29}Si MAS NMR and ^{13}C CP MAS NMR spectra were recorded at room temperature using a Bruker MSL-300 spectrometer. The ^{29}Si resonance frequency used was 59.595 MHz, and the rotor was spun at 3.0 KHz. The radio frequency field was 37.0 KHz, corresponding to a $\pi/3$ pulsewidth of $4.5\ \mu\text{s}$, and the recycle time was 2 s. Q_8M_8 was used as a second reference for the ^{29}Si chemical shift. The ^{13}C resonance frequency was 75.468 MHz, and the rotor was spun at 4.0 KHz. The radio frequency field was 50 KHz, corresponding to a $\pi/2$ pulsewidth of $5\ \mu\text{s}$, and the recycle time was 2 s. For each measurement 2000–6000 spectra were accumulated. Adamantane was used as a second reference for the ^{13}C chemical shift. TG/DTG/DTA measurements were carried out from room temperature to $500\ ^\circ\text{C}$ using a PTC-10 A thermal analyzer in an air flow of $70\ \text{ml}/\text{min}$ at a heating rate of $5\ ^\circ\text{C}/\text{min}$. The sample load was 10 mg and the sensitivity of TG and DTA used were 0.01 mg and $\pm 25\ \mu\text{V}$, respectively.

3. Results and Discussion

3.1. XRD PATTERNS

Figure 1 shows the XRD patterns over a wide scanning range for silicalite samples with various loadings of *p*-xylene. As the amount of *p*-xylene adsorbed in the zeolite is increased, the gradual decrease in the intensities of the low angle peaks on the patterns is obvious. At the same time, the intensities of the peaks at about $23^\circ(2\theta)$ are enhanced as the loading of *p*-xylene is increased from 0 to about 4 molecules/u.c. When the loading > 5.2 molecules/u.c., the peak intensity is reduced as the *p*-xylene loading is further increased. The transition of the intensity is caused by the various structural factors of the zeolite with different *p*-xylene loadings.

XRD patterns of silicalite with various loadings in selected scanning ranges are shown in Figure 2. As reported by Fyfe *et al.* [14], the loss of the doublet splitting of the peaks at 24.4° , 29.3° and $48.3^\circ(2\theta)$ when the *p*-xylene loading are > 1 molecule/u.c., corresponds to a transition from monoclinic to orthorhombic symmetry. But in the range of 23° to $24^\circ(2\theta)$, the changes of the peaks are more complicated. If the loading > 1.1 molecules/u.c., a triple peak in the 2θ range of 23.0° to 23.3° immediately combine, and another triple peak in the 2θ range of 23.7° to 23.9° becomes a double peak at 23.7° and $23.9^\circ(2\theta)$, respectively. When the *p*-xylene loadings are > 5.2 molecules/u.c., the peak at $23.2^\circ(2\theta)$ splits. At the same time the double peaks at about $23.8^\circ(2\theta)$ combine. Van Koningsveld *et al.* [13] have reported that the space group of silicalite with loadings < 4 molecules/u.c. can be treated as *Pnma*, which is the same as that of the as-synthesized MFI type zeolite. The simulated XRD patterns from single crystal structure data and the

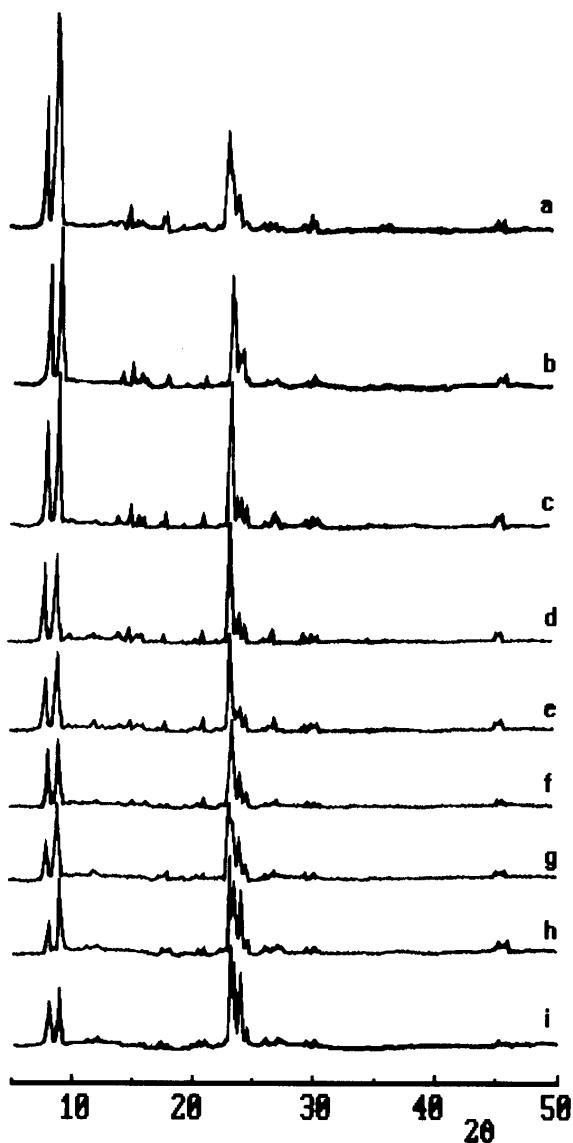


Figure 1. XRD patterns in a wide scanning range for silicalite with various numbers of *p*-xylene molecules per unit cell. (a) 0, (b) 1.1, (c) 2.0, (d) 3.4, (e) 3.9, (f) 5.2, (g) 5.9, (h) 7.2, (i) 7.8.

Miller index for each peak can be found in reference [33]. So the Miller index of the peaks at 23.2° , 23.7° , and 23.9° (2θ) are [501], [151], and [303] respectively. Figure 3 illustrates the changes of the peak positions in the range of 23° to 24° (2θ) in detail. The sudden breaks on the curves of peak position indicate that a transition of space group has occurred with 5 to 6 molecules/u.c. of *p*-xylene loading. Also,

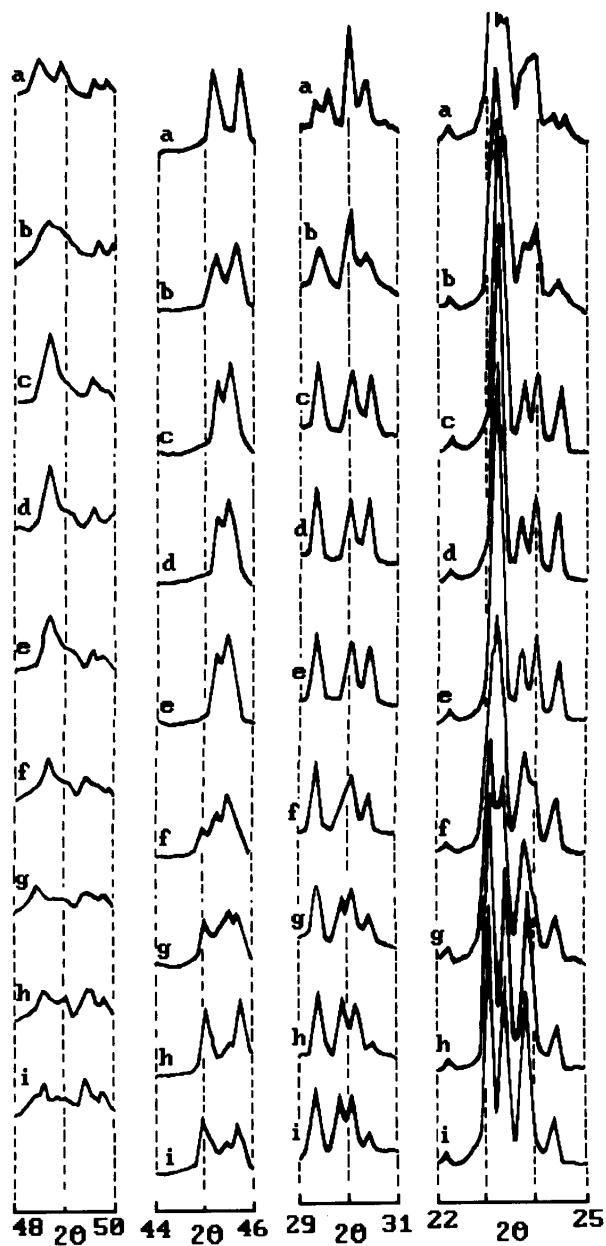


Figure 2. XRD patterns in selected scanning ranges for silicalite with various numbers of *p*-xylene molecules per unit cell. (a) 0, (b) 1.1, (c) 2.0, (d) 3.4, (e) 3.9, (f) 5.2, (g) 5.9, (h) 7.2, (i) 7.8.

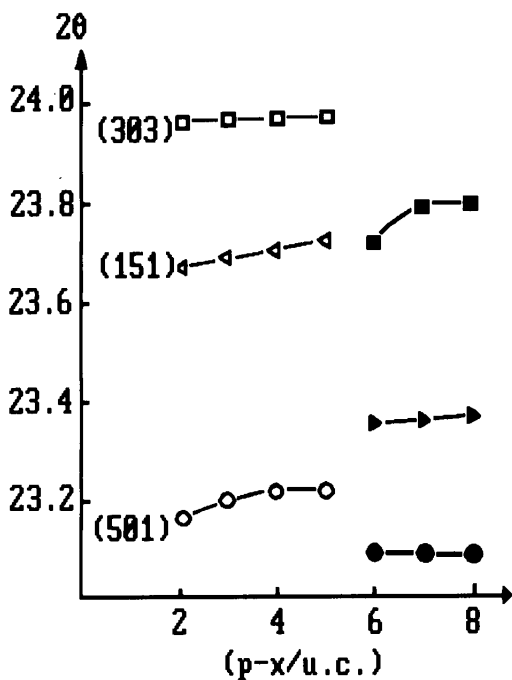


Figure 3. Shifts of XRD peaks for silicalite vs. *p*-xylene molecules per unit cell.

the [10 0 0] peak at $45.2^\circ(2\theta)$ moves to higher angle as the loading is increasing from 0 to 3.9 molecules/u.c. If the loading >5.2 molecules/u.c., the shift of the [10 0 0] peak is negligible. This indicates that the cell constant along the *a*-axis firstly constricts, and then remains invariable. The [0 10 0] peak at $45.7^\circ(2\theta)$ shifts obviously towards a lower angle with increasing *p*-xylene loading from 0 to 5.2 molecules/u.c. Then the peak moves to a higher angle as the loading increases. This indicates that the cell parameter along the *b*-axis of the zeolite has a transition from expansion to constriction. The phenomenon of the cell constant changing with the *p*-xylene loading is basically consistent with the results of reference [16].

3.2. HIGH RESOLUTION ^{29}Si MAS NMR SPECTRA

Figure 4 shows the high resolution ^{29}Si MAS NMR spectra of samples with different loadings of *p*-xylene. The appearance of the 16 independent, well-resolved resonance peaks proves that the silicalite sample used in this study possesses a perfect framework of monoclinic symmetry [30, 35]. When the *p*-xylene loadings are >1 molecule/u.c., the number of resonance peaks decreases to 8, which is evidence of the occurrence of the monoclinic/orthorhombic transition. Two spectra with loadings of 2.2 and 3.6 molecules/u.c. (see Figure 4d,e) are similar to that of the samples with a loading $8 \mu\text{L}$ and $40 \mu\text{L/g}$ reported by C. A. Fyfe *et al.* [14].

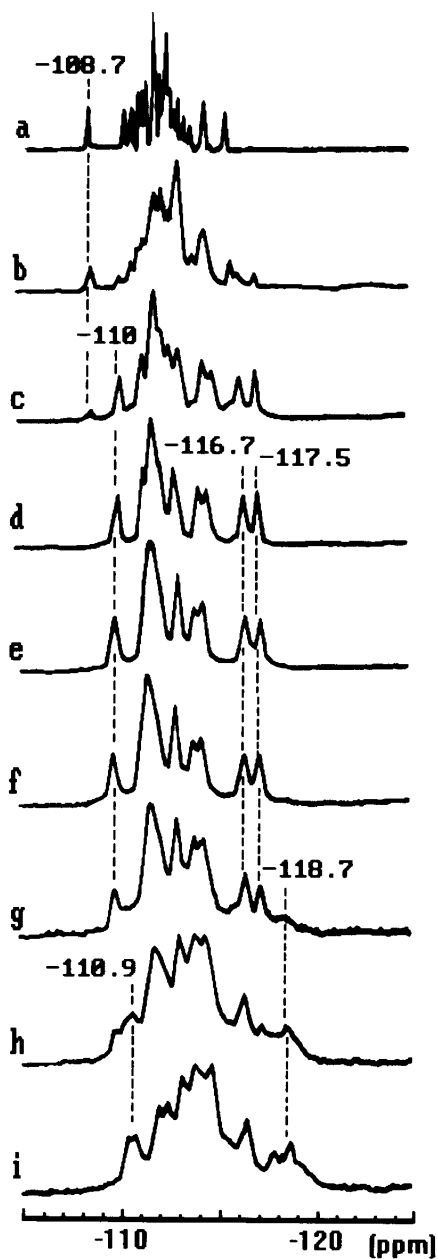


Figure 4. ^{29}Si MAS NMR spectra of silicalite with various numbers of *p*-xylene molecules per unit cell. (a) 0, (b) 0.3, (c) 0.9, (d) 2.2, (e) 3.6, (f) 4.4, (g) 5.8, (h) 6.5, (i) 7.7.

Our spectra have better resolution, however. At the same time, the resolution of the resonance peaks becomes poorer with increasing loading, and the peak at -108.7 ppm disappears and three new peaks at about -110 ppm, -116.7 and -117.5 ppm appear. The same type of ^{29}Si MAS NMR spectrum remains until the *p*-xylene loading reaches 5.8 molecules/u.c., which means that in the loading range of 1 to 5.8 molecules/u.c. the zeolite crystal structure belongs to a specific space group of orthorhombic symmetry [14]. This *p*-xylene/silicalite associate is designated as associate-I. When the *p*-xylene loading is above 5.8 molecules/u.c., the -110 ppm peak becomes weaker, and finally disappears. Meanwhile two new peaks appear at -110.9 ppm and -118.7 ppm. The variation in spectrum can be recognized as a sign for associate-I changing to another space group of orthorhombic symmetry, and this new *p*-xylene/silicalite associate is designated as associate-II. The results of ^{29}Si MAS NMR studies are consistent with those of XRD measurements.

There is an interesting phenomenon in the ^{29}Si MAS NMR spectra. The resonance peaks shift progressively to high field with increasing loading of *p*-xylene. The cause of this change in chemical shift is most likely the interaction between the framework and the adsorbed *p*-xylene. It is known that the framework of silicalite is constructed of $[\text{SiO}_4]$ tetrahedra linked by sharing O^{2-} . The Si—O distance and O—Si—O angle change only a little with the transition of space group [13], whereas the influence of the interaction between the framework O^{2-} and the adsorbed molecules on the chemical shift is more important. Since the radius of an oxygen atom is much larger than that of a silicon atom, the whole framework surface is actually covered with O^{2-} . The average distance between two neighboring atoms of oxygen in the silicalite framework is 0.149 nm, which is very close to 0.154 nm, the average distance between two neighboring atoms of carbon in hydrocarbons. The O^{2-} of the silicalite interacts with a molecule of *p*-xylene, partly changing the distribution of electrons in C—H groups, and causes the formation of an instantaneous dipole moment, inducing electrical polarity. Therefore the van der Waals force plays a role in the interaction. At high loading a *p*-xylene/*p*-xylene associate is formed in the channel interactions. Hence, the chemical environment of O^{2-} and the neighboring Si atom is changed considerably after *p*-xylene adsorption, which leads to the upfield shift of the peaks and the broadening of the resonance peaks with increasing loading.

As far as we know, the high resolution ^{29}Si MAS NMR spectra of silicalite with various *p*-xylene loadings in this study are the first report in the literature. The interaction between *p*-xylene and the silicalite framework is very clearly shown on these spectra. It gave reliable and important evidence of the formation and the characters of the two types of associates with different space groups. Comparing Figure 4 with Figures 1 and 2, it can be seen that the ^{29}Si MAS NMR spectra are more sensitive than XRD patterns in identifying the formation of two types of associate with different space groups of orthorhombic symmetry. The NMR spectra are simpler and more characteristic than the XRD patterns.

3.3. ^{13}C CP MAS NMR

^{13}C CP MAS NMR spectra of *p*-xylene loaded on silicalite are given in Figure 5. The high resolution spectra are the first to be observed and reported. Two broad ^{13}C resonance peaks appear at 127.9 and 133.9 ppm on the spectra when the *p*-xylene loading is in the range of 0.9 to 6.5 molecules/u.c. (see Figure 5a–e). The intensities of the peaks at 127.9 and 133.9 ppm become stronger and their resolution better (see Figure 5f) when the *p*-xylene loading increases to 7.0 molecules/u.c. Three additional peaks, two near 18.7 ppm and one near 133.9 ppm, are observed in the spectra of the sample with a loading of 7.3 molecules/u.c. (see Figure 6a). Eventually a well resolved spectrum can be seen in Figure 6b with up to nine distinct resonances at 17.7, 18.8, 19.8, 126.8, 128.1, 129.0, 129.8, 132.9 and 134.0 ppm, respectively, for the sample with a loading of 8.2 molecules/u.c. The variations in the spectra show that the *p*-xylene molecules change from low-ordered to high-ordered as the adsorbed *p*-xylene loading in the zeolite is increased. This observation is consistent with the results of single crystal studies on the *p*-xylene/HZSM-5 complex by van Koningsveld [13].

The ^{13}C CP MAS NMR spectrum of pure *p*-xylene has three clearly resolved resonance lines at 20.9 ppm (carbon atoms in methyl group), 127.2 and 134.6 ppm (carbon atoms in aromatic ring), respectively. For the samples with low *p*-xylene loading the presence of the two broad peaks at 127.9 and 133.9 ppm show that there are strong interactions between the *p*-xylene molecules and the zeolite framework. On the other hand, the resonance for the carbon atom in the methyl group shifts about 2 ppm to high field (18.7 ppm), which also indicates that the adsorbed *p*-xylene molecules are more restricted in the zeolite channels and the hydrogen atoms in the methyl group of the adsorbed molecules cannot rotate freely along the C—C axis.

For the samples with high *p*-xylene loading the resonance peaks at 19.8, 126.8 and 132.9 ppm in the ^{13}C spectra are probably associated with the *p*-xylene molecules adsorbed on the external surface of silicalite. Because of 8 molecules/u.c. for the saturated sorption, there are small amounts of *p*-xylene molecules out of the zeolite channels when the loading = 8.2 molecules/u.c. The other resonance peaks with ^{13}C chemical shifts at 17.7 and 18.8 ppm for the carbon atoms of the methyl group and at 128.1, 129.0, 129.8 and 134.0 ppm for the carbon atoms of the aromatic ring indicate that there are at least another two different positions for the adsorbed *p*-xylene molecules. From the very accurate XRD data of Koningsveld [13], the two positions may correspond to the channel intersection and the sinusoidal channel in the zeolite. It is obvious that the *p*-xylene molecules in the sinusoidal channels should be restricted more strongly than those at other positions [13, 25]. With low loading the adsorbed molecules are more dispersed and low-ordered. By contrast, in the channel intersections there is more space for the adsorbed *p*-xylene molecules to interact with each other via hydrogen bonding to form a high-ordered *p*-xylene/*p*-xylene complex at high loading. The difference

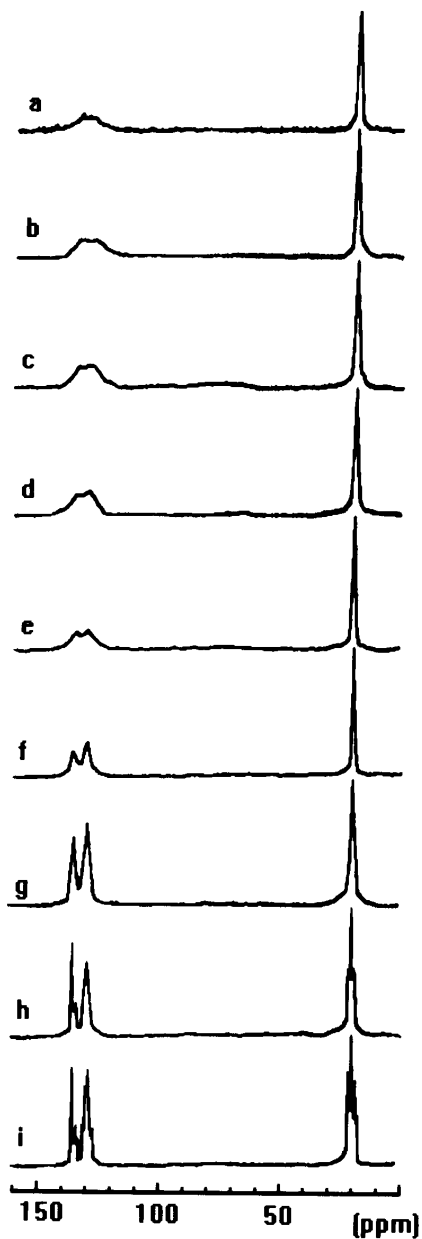


Figure 5. ^{13}C CP MAS NMR spectra of *p*-xylene adsorbed on silicalite with the loading of: (a) 0.9, (b) 3.5, (c) 5.3, (d) 5.8, (e) 6.5, (f) 7.0, (g) 7.2, (h) 7.3, (i) 8.2 molecules/u.c.

in the interactions of the *p*-xylene molecules with the zeolite framework and with each other is responsible for the variation in the chemical shifts.

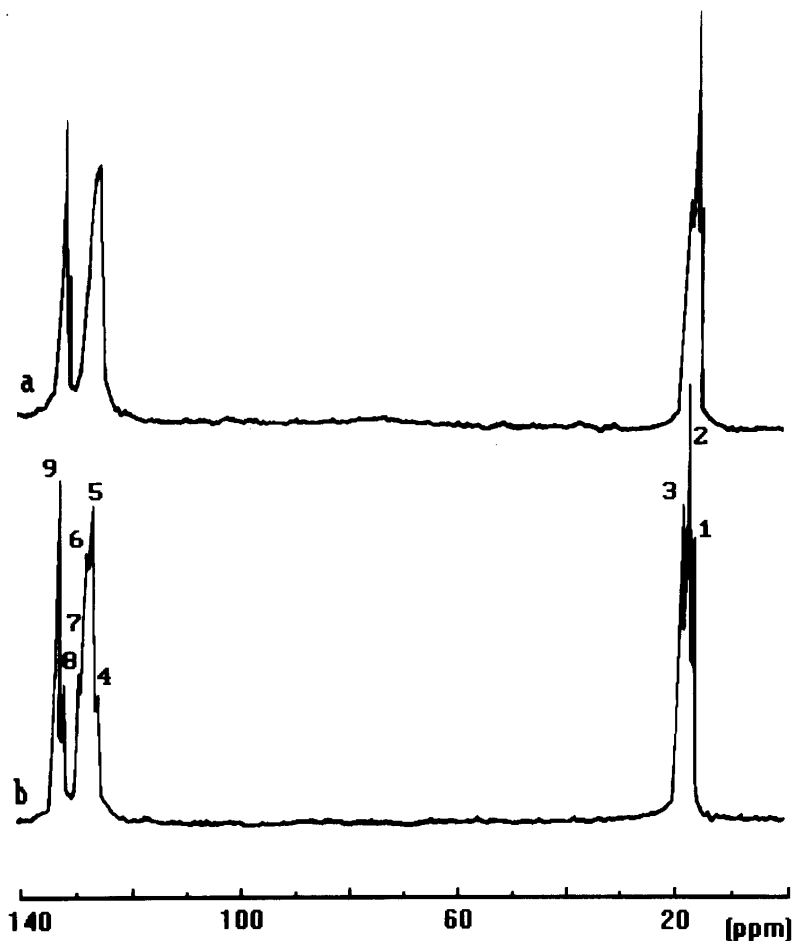


Figure 6. High resolution ^{13}C CP MAS NMR spectra of *p*-xylene adsorbed on silicalite with the loading of (a) 7.3, and (b) 8.2 molecules/u.c. The chemical shifts (ppm) of the peaks. (1) 17.7, (2) 18.8, (3) 19.8, (4) 126.8, (5) 128.1, (6) 129.0, (7) 129.8, (8) 132.9, (9) 134.0.

Looking carefully at the results of the high resolution ^{13}C CP MAS NMR spectra and the ^{29}Si MAS NMR spectra, one notices that the space group of the zeolite and the chemical state of the *p*-xylene molecules adsorbed are related. It can be suggested that the change in space group with high *p*-xylene loading is induced by the interactions of the *p*-xylene molecules with the zeolite framework and with each other.

3.4. TG/DTG/DTA

It was known that there are two steps that occur in the *p*-xylene adsorption isotherms of silicalite at 60 °C or 70 °C [2, 16]. One step is related to the *p*-xylene loading of

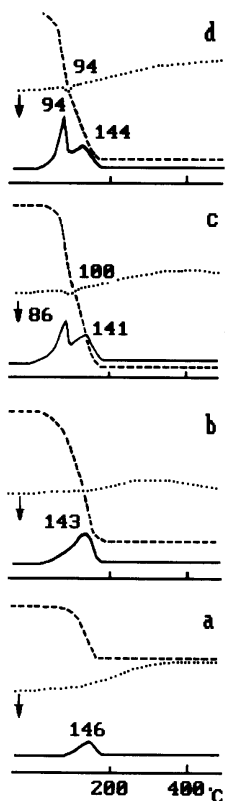


Figure 7. TG/DTG/DTA spectra of *p*-xylene on silicalite with loadings of (a) 1.6, (b) 3.9, (c) 6.0, (d) 7.3 molecules/u.c. - - - - TG; — DTG; ····· DTA; ↓ endothermic effect.

3.9 ± 0.1 molecules/u.c., and the second related to the loading of 7.8 ± 0.2 molecules/u.c. These steps are suggestive of a solid phase change. The TG/DTG/DTA curve at high *p*-xylene loading in silicalite was reported in our earlier work [20–22]. It shows two weight loss peaks on the DTG curve. The shape of the TG curve is similar to the temperature programmed desorption curves of C_6 and C_7 *n*-alkanes from silicalite [18]. It was explained that some kind of phase transition takes place. Now we report the TG/DTG/DTA curves of various *p*-xylene loadings on silicalite. Only one weight loss peak appears on the DTG curves of the samples with loadings of 1.6 and 3.9 molecules/u.c. (see Figure 7a,b). The temperature of the weight loss peak is at about 140 °C. There are two weight loss peaks at the temperatures of about 90 °C and 140 °C on the DTG curves of the samples with loadings of 6.0 and 7.4 molecules/u.c. (see Figure 7c,d). The peak at about 90 °C is sharper than the one at about 140 °C, which indicates that the desorption rate of the first process is higher. The temperature for complete desorption of *p*-xylene is about 180 °C. The heat of desorption is negligible when the loadings are < 4 molecules/u.c. An endothermic desorption peak is obvious on the DTA curves at a temperature of

2. D.H. Olson, G.T. Kokotallo, S.L. Lawton, and W.M. Meier: *J. Phys. Chem.* **85**, 2238 (1981).
3. Y.H. Ma, T.D. Tong, L.B. Sand, and L.Y. Hou: *New Developments in Zeolite Science Technology* (Proceeding of the 7th International Zeolite Conference, Eds. Y. Murakami, A. Lijima and J.W. Ward), pp. 531, Kadansha Ltd. (1986).
4. D.M. Ruthven, M. Eic, and E. Richard: *Zeolites* **11**, 647 (1991).
5. S.G. Hill and D. Seddon: *Zeolites* **11**, 699 (1991).
6. C. G. Pope: *J. Phys. Chem.* **90**, 835 (1986).
7. H. Karsli, A. Gulfaz, and H. Yucel: *Zeolites* **12**, 728 (1992).
8. H.-J. Doelle, J. Heering, L. Riekert, and L. Marosi: *J. Catal.* **71**, 27 (1981).
9. D. Shen and L.V.C. Rees: *Zeolites* **11**, 684 (1991).
10. H. Thamm: *J. Phys. Chem.* **92**, 193 (1988).
11. B.F. Mentzen: *Mat. Res. Bull.* **30**, 1333 (1995).
12. B.F. Mentzen and F. Lefebvre: *Mat. Res. Bull.* **30**, 613 (1995).
13. H. van Koningsveld, F. Tuinstra, H. van Bekkum and J.C. Jansen: *Acta Crystallogr.* **B45**, 423 (1989).
14. C.A. Fyfe, G.J. Kennedy, C.T. De Schutter, G.T. and Kokotailo: *J. Chem. Soc. Chem. Commun.* 541 (1984).
15. R.L. Portsmouth and L.F. Gladden: *J. Chem. Soc. Chem. Commun.* 512 (1992).
16. B.F. Mentzen and P. Gelin: *Mat. Res. Bull.* **30**, 373 (1995).
17. B. Smit and T.L.M. Maesen: *Nature* **374**, 42 (1995).
18. W.J.M. van Well, J.P. Wolthuizen, B. Smit, J. H. C. van Hooff, and R.A. van Santen: *Angew. Chem. Int. Ed. Engl.* **34**, 2543 (1995).
19. Y.C. Long, H.W. Jiang, and H. Zeng: *J. Fudan Univ.* **33**, 101 (1994).
20. Y.C. Long, H.W. Jiang, and H. Zeng: *Acta Chimica Sinica* **54**, 545 (1996).
21. Y.C. Long, H.W. Jiang, and H. Zeng: *Progress in Zeolite and Microporous Materials*, Studies in Surface Science and Catalysis, vol. 105 (Proc. of 11th IZC); Eds. H. Chou et al., Elsevier Science BV, pp. 787 (1997).
22. Y.C. Long, H.W. Jiang, and H. Zeng: *Langmuir* (to be published).
23. E.L. Wu, S.L. Lawton, D.H. Olson, A.C. Jr. Rohrman, and G.T. Kokotallo: *J. Phys. Chem.* **83**, 2777 (1979).
24. W.C. Conner, R. Vincent, P. Man, and J. Fraissard: *Catal. Lett.* **4**, 75 (1990).
25. J.A. Muller and W.C. Conner: *J. Phys. Chem.* **97**, 1451 (1993).
26. J.M. Chezeau, L. Delmott, T. Hasebe, and N.B. Chanh: *Zeolites* **11**, 729 (1991).
27. H. Van Koningsveld, H. Van Bekkum, and J.C. Jansen: *Acta Crystallogr.* **B43**, 127 (1987).
28. H. Van Koningsveld, J.C. Jansen, and H. Van Bekkum: *Zeolites* **10**, 235 (1990).
29. C.A. Fyfe, H. Grondy, Y. Feng, and G.T. Kokotailo: *Chem. Phys. Lett.* **173**, 211 (1990).
30. C.A. Fyfe, J.H. O'Brien, and H. Strobl: *Nature* **326**, 281 (1987).
31. H. Zeng, H. W. Jiang, and Y. C. Long: *Acta Physico-Chimica Sinica* **11**, 252 (1995).
32. Y.C. Long, Y.J. Sun, T. L. Wu, L.P. Wang, M. Qian, and L. Fei: *CN Patent Appl. No.* 92 1 13807.5 (1992).
33. M.M.J. Treacy, J.B. Higgins, and R. von Ballmoos: *Collection of Simulated XRD Powder Patterns for Zeolites*, Third Revised Edition, Published on behalf of the Structure Commission of the International Zeolite Association, Amsterdam: Elsevier, pp. 522 (1996).
34. I. Suzuki, S. Nambq, and T. Yashima: *J. Catal.* **81**, 485 (1983).
35. Y.J. Sun, Y.F. Huang, T.L. Wu, L.P. Wang, L. Fei, and Y.C. Long: *Acta Chemica Sinica* **52**, 573 (1994).